

Marc Jerónimo Pérez y Roperó
13-938-311

P-release kinetic as a predictor for P-availability in the STYCS Trials

Master's Thesis

Master's Degree Programme in Agricultural Sciences
Plant Nutrition Group
Swiss Federal Institute of Technology (ETH) Zurich

Supervision

Prof. Dr. Emmanuel Frossard
Dr. Frank Liebisch

Abstract

Hier kommt das Abstract

Table of contents

1	Abstract	1
2	Introduction	1
2.1	The Complexity of Phosphorus	1
2.2	From Static Measurements to Dynamic Understanding	1
2.3	Objectives and Research Questions	2
2.3.1	Research Questions and Hypotheses	2
3	Materials and Methods	3
3.1	The Long-Term Phosphorus Fertilization Experiment	3
3.2	Experimental Sites	3
3.3	Phosphorus Desorption Kinetics	4
3.3.1	Original Method of Flossmann and Richter (1982)	4
3.3.2	Adapted Kinetic Protocol for This Study	4
3.4	Statistical Analysis	4
3.4.1	Software and Statistical Environment	4
3.4.2	Modeling of Desorption Kinetics	4
3.4.3	Comparative Modeling of Soil and Agronomic Parameters	5
3.4.4	Model Assumptions and Diagnostics	5
4	Results	6
4.1	Establishment of the P-Desorption Kinetic Model	7
4.1.1	Initial Approach: Failure of the Linearized Model	7
4.1.2	Final Approach: Successful Non-Linear Model	7
4.2	Comparison with Isotopic Exchange Kinetics (IEK) {#sec-comparison-with-isotopic-exchange-kinetics-(iek)}	8
4.3	Effects of Fertilization on Agronomic and Soil Parameters	9
4.3.1	Agronomic Responses to P Fertilization	9
4.3.2	Soil P Parameters as a Function of P Fertilization	11
4.4	Predicting P Parameters from Soil Properties	12
4.5	Predictive Modeling of Agronomic Outcomes	13
4.5.1	Predicting Site-Normalized Yield (Y_{norm})	13
4.5.2	Predicting National-Normalized Yield (Y_{rel})	14
4.5.3	Predicting P-Uptake (P_{up})	15
4.5.4	Predicting P-Balance (P_{bal})	16
5	Discussion	17
5.1	Hypothesis 1: The Nuanced Role of Standard Soil Tests	17
5.2	Hypothesis 2: Characterizing P Desorption Kinetics	18
6	Conclusion	20
7	Acknowledgments	20
8	Legal Disclosure	20
9	References	21
10	Appendix	23

11 Supplements	23
List of Figures	24
List of Tables	25

1 Abstract

2 Introduction

2.1 The Complexity of Phosphorus

Phosphorus (P) is an essential macronutrient for all known life, forming a critical part of DNA and energy-transfer molecules (Berg et al., 2019; National Institutes of Health, Office of Dietary Supplements, 2023; Nelson et al., 2021). In soils—where organic, mineral, and aqueous phases interface—its behavior is complex. In the presence of oxygen, P exists almost exclusively as orthophosphate (PO_4^{3-}) and its protonated forms (HPO_4^{2-} or $H_2PO_4^-$), depending on the soil pH (Brady & Weil, 2016; Sparks, 2003). These dissolved phosphate species are highly reactive; they are subject to adsorption onto the surfaces of clays and oxides and can precipitate with cations like calcium, iron, and aluminum to form minerals with low solubility (Bohn et al., 2002; Hinsinger, 2001; Sposito, 2008). Consequently, while total soil P concentrations can be substantial, often ranging from 200 to 3000 mg kg⁻¹, the concentration of orthophosphate in the soil solution—the form directly acquired by plant roots—is typically minuscule, often in the range of 0.001 to 1 mg L⁻¹. This vast difference between the total phosphorus stock and the infinitesimally small plant-available pool represents a central challenge for global agricultural productivity (Brady & Weil, 2016; Holford, 1997; Sposito, 2008). This creates a profound agronomic and environmental dilemma: while the majority of applied P fertilizer is rapidly immobilized in the soil and remains unavailable to crops, the fraction that is lost from fields via runoff and erosion becomes a potent environmental pollutant. This fugitive P is a primary driver of eutrophication in freshwater ecosystems, which are often naturally P-limited (Sharpley et al., 2003).

Soil organic matter (SOM) adds another layer of complexity to these interactions. Organic acids released during the decomposition of SOM can compete with phosphate for the same adsorption sites on mineral surfaces, which can increase P concentrations in the soil solution. Furthermore, humic substances can form stable complexes with cations like Al³⁺ and Fe³⁺, preventing them from precipitating phosphate and thereby enhancing its availability (Gerke, 2010; Stevenson, 1994).

2.2 From Static Measurements to Dynamic Understanding

To manage this challenge, soil testing methods were developed to estimate plant-available phosphorus. These tests are designed to measure two key components of P availability: the **intensity factor**, which is the concentration of P in the soil solution at a given moment, and the **capacity factor**, which represents the pool of weakly adsorbed P that can readily replenish the soil solution. Traditional methods used in Switzerland and the surrounding DACH region, such as extraction with CO₂-saturated water or ammonium acetate EDTA (AAE10), are designed to estimate the size of this readily available P pool (the capacity factor) (Forschungsanstalt für Agrarökologie und Landbau (FAL), 1996; Schofield, 1955; Verband Deutscher Landwirtschaftlicher Untersuchungs- und Forschungsanstalten (VDLUFA), 2000). While these tests are invaluable for basic fertility assessment, they do not capture the dynamic nature of P supply. A crucial missing piece of information is the rate at which P is replenished into the soil solution from the solid phase after being taken up by plant roots. This replenishment rate, or **“kinetic factor”**, is vital for sustaining crop growth, especially during periods of high demand (Frossard et al., 2000).

The importance of these dynamics is not a new concept. As early as 1982, **Flossmann and Richter** argued that characterizing the kinetics of P release was essential for refining fertilizer recommendations beyond what static tests alone could offer (Flossmann & Richter, 1982). Modern research has reinforced this view, showing that fertilization strategies based solely on maintaining a critical soil test P (STP) concentration can be inefficient (McDowell & Sharpley, 2001; Rowe et al., 2016). In Switzerland, this has led to the accumulation of “legacy P” in many agricultural soils, and understanding the release kinetics of this legacy P is key to both improving nutrient efficiency and protecting water quality (Hirte et al., 2018). Furthermore, critical STP levels are not

constant; they are influenced by pedoclimatic factors like soil texture and temperature, making a “one-size-fits-all” approach to fertilization suboptimal (Bell et al., 2013; Hirte, Richner, et al., 2021; Sims & Sharpley, 2005).

2.3 Objectives and Research Questions

An ideal set of parameters for phosphorus (P) management must move beyond simple agronomic sufficiency to encompass both environmental stewardship and the biophysical realities of nutrient acquisition by plants. To be truly effective, such parameters must: (1) be sensitive to changes in the soil P status resulting from fertilizer inputs and crop removal (the P balance) (Johnston et al., 2001); (2) correlate with the risk of P loss to the environment (P export) (Sharpley et al., 2000); and (3), most critically, reflect the kinetic nature of P supply to plant roots, which is governed by the slow diffusion of phosphate in the soil solution (Kuang et al., 2012; Nye & Tinker, 2000).

This thesis hypothesizes that kinetic parameters describing P desorption, derived from a simple laboratory extraction, can serve as effective predictors for agronomic outcomes. To test this, soils were sourced from the long-term Swiss agricultural experiment STYCS (Hirte, Stüssel, et al., 2021), which provides an ideal platform for this research. The experiment’s multi-decade history has established stable P equilibria across a wide and deliberately created gradient of P availability (from 0% to 167% of recommended fertilization). This allows for robust modeling of crop responses. Furthermore, the trial encompasses six sites with diverse pedoclimatic conditions, ensuring that any findings have broad applicability across different Swiss agricultural landscapes. This study employs a modified version of the Flossmann & Richter kinetic test to derive the desorption rate (k) and the desorbable P pool (P_{desorb}). The performance of these new kinetic parameters will be compared against standard STP methods (P_{CO_2} and P_{AAE10}) by addressing the following research questions:

2.3.1 Research Questions and Hypotheses

2.3.1.1 Research Question 1: How well do standard soil test P (STP) methods predict agronomic outcomes and how do they relate to fundamental soil properties?

- **Hypothesis 1a (Agronomic Performance):** The standard STP methods (P_{CO_2} and P_{AAE10}), which measure the P *capacity* (the size of the readily available pool), will show a significant correlation with the P-Balance, as this is directly influenced by P inputs (Johnston et al., 2001). However, they will be weak predictors of relative crop yield and P-uptake, as these agronomic outcomes are more dependent on the *rate* of P supply throughout the growing season (Hirte, Stüssel, et al., 2021).
- **Hypothesis 1b (Relation to Soil Properties):** The measured STP values will be positively correlated with soil clay and organic carbon content, reflecting the greater number of sorption sites in these soils (Brady & Weil, 2016). Conversely, the P_{AAE10} measurement will be negatively correlated with soil pH, particularly in soils with a $pH > 6.8$, due to the chelation of Ca^{2+} and Mg^{2+} by the EDTA in the extractant, which reduces its effectiveness (Forschungsanstalt für Agrarökologie und Landbau (FAL), 1996).

2.3.1.2 Research Question 2: Can P desorption kinetics be reliably characterized for the diverse soils of the STYCS trial, and how do the derived kinetic parameters relate to soil properties?

- **Hypothesis 2a (Methodological Feasibility):** The P desorption process in the STYCS soils will follow a first-order kinetic model. However, the original linear estimation method proposed by Flossmann & Richter (1982) may be inaccurate because it relies on a potentially overestimated desorbable P pool (P_{desorb}). A non-linear modeling approach will provide more robust and replicable estimates of both the desorption rate constant (k) and the desorbable P pool (P_{desorb}) (Kuang et al., 2012).

- **Hypothesis 2b (Relation to Soil Properties):** The kinetic parameters will be significantly influenced by soil composition. The desorbable P pool (P_{desorb}) is expected to correlate positively with clay and organic matter content, which provide sorption surfaces. The rate constant (k) is expected to be influenced by pH, as the speciation of orthophosphate changes, affecting its interaction with mineral surfaces and its mobility (Sparks, 2003).

2.3.1.3 Research Question 3: Can kinetic parameters significantly improve the prediction of agronomic outcomes compared to standard static STP methods?

- **Hypothesis 3 (Improved Predictive Power):** Because plant P uptake is fundamentally limited by the slow diffusion of phosphate to the root surface, a dynamic measure is required for accurate prediction (Nye & Tinker, 2000). Therefore, a model incorporating the kinetic parameters (k and P_{desorb}), which together describe the replenishment rate of the soil solution, will explain a significantly greater proportion of the variance in relative yield and P-uptake compared to models based solely on the static STP measurements (Fardeau et al., 1991; Frossard et al., 2000).

3 Materials and Methods

3.1 The Long-Term Phosphorus Fertilization Experiment

The soil samples for this thesis originate from a set of six long-term field trials in Switzerland, established by Agroscope between 1989 and 1992. The primary objective of these experiments was to validate and re-evaluate Swiss phosphorus (P) fertilization guidelines by assessing long-term crop yield responses to varying P inputs across different pedoclimatic conditions. A detailed description of the experimental design and site characteristics can be found in Hirte, Richner, et al. (2021).

The experiment was set up as a **completely randomized block design** with four field replications at each site. The core of the experiment consists of six fixed-plot treatments representing different P fertilization levels, which were applied annually as superphosphate before tillage and sowing. These levels were based on percentages of the officially recommended P inputs: 0% (Zero), 33% (Deficit), 67% (Reduced), 100% (Norm), 133% (Elevated), and 167% (Surplus).

3.2 Experimental Sites

The six experimental sites are located in the main crop-growing regions of Switzerland: **Rümlang-Altwi (ALT)**, **Cadenazzo (CAD)**, **Ellighausen (ELL)**, **Grabs (GRA)**, **Oensingen (OEN)**, and **Zurich-Reckenholz (REC)**. The key soil properties are summarized below.

Table 1: Soil characteristics of the six long-term experimental sites. Data adapted from Hirte et al. (2021).

Site	Soil Type (WRB)	Clay (%)	Sand (%)	Organic C (g/kg)	pH (H ₂ O)
ALT	Calcaric Cambisol	22	48	21	7.9
CAD	Eutric Fluvisol	8	40	14	6.3
ELL	Eutric Cambisol	33	31	23	6.6
GRA	Calcaric Fluvisol	17	34	16	8.3
OEN	Gleyic-calc. Cambisol	37	32	24	7.1
REC	Eutric Gleysol	39	25	27	7.4

Soil samples for this thesis were collected in the year 2022 from the topsoil layer (0-20 cm).

3.3 Phosphorus Desorption Kinetics

The analysis of phosphorus (P) desorption kinetics was based on the principles of sequential extraction established by (Flossmann & Richter, 1982). The original method is described below, followed by the specific protocol adapted for this study.

3.3.1 Original Method of Flossmann and Richter (1982)

The foundational method aims to characterize the P replenishment capacity of the soil. The procedure is as follows:

1. **Removal of Soluble P:** 17.5 g of air-dried soil is shaken with 350 ml of deionized water for one hour at 120 Hz in a horizontal soil-shaker. The suspension is centrifuged at 4000 rpm for 15 minutes and the supernatant is decanted to remove the readily soluble P fraction.
2. **Kinetic Extraction:** The remaining soil pellet is resuspended with another 350 ml of deionized water. Subsamples of the suspension are taken at specific time intervals (e.g., 10, 30, and 120 minutes).
3. **Analysis:** The P concentration in the subsamples is determined colorimetrically.

3.3.2 Adapted Kinetic Protocol for This Study

For this thesis, the original method was modified to capture the desorption process with a higher temporal resolution.

1. **Pre-washing to Remove Soluble P:** A pre-washing step was performed to remove the readily soluble P fraction. 10 g of air-dried soil was suspended in 200 ml of deionized water and shaken for 60 minutes at 120 Hz. The suspension was then centrifuged for 15 minutes at 4000 rpm, and the supernatant containing the soluble P was discarded.
2. **Kinetic Extraction:** The remaining soil pellet was resuspended in 200 ml of fresh deionized water. The suspension was shaken continuously, and subsamples were taken at eight time points to generate a detailed kinetic curve: **2, 4, 10, 15, 20, 30, 45, and 60 minutes**.
3. **Analysis:** Each subsample was immediately filtered. The concentration of orthophosphate in the filtered extracts was determined colorimetrically using the **malachite green method** (Van Veldhoven & Mannaerts, 1987).

3.4 Statistical Analysis

3.4.1 Software and Statistical Environment

All data processing, statistical modeling, and visualization were conducted using the R programming language (v. 4.2.2) (R Core Team, 2022). The primary packages used for the analysis were: - **nlme** (Pinheiro et al., 2022) for fitting the non-linear mixed-effects models to the kinetic data. - **lme4** (Bates et al., 2015) and **lmerTest** (Kuznetsova et al., 2017) for fitting and testing the linear mixed-effects models for agronomic and soil property analyses. - **mlr3** (Lang et al., 2019) for the systematic feature selection and model validation workflow.

3.4.2 Modeling of Desorption Kinetics

To derive the kinetic parameters, a non-linear mixed-effects model was implemented using the **nlme** package. This approach was chosen to simultaneously estimate the rate constant (k) and the maximum desorbable P (P_{desorb}) for each soil sample. The model was fitted to the exact solution of the first-order rate equation:

$$P(t) = P_{desorb} \times (1 - e^{-k \times t'})$$

Where $P(t)$ is the P concentration at time t , and t' is an adjusted time ($t_{min} + 3 \text{ min}$) to account for the rapid initial dissolution of P that occurs before the first measurement. In this mixed-effects framework, the overall mean values for P_{desorb} and k were modeled as **fixed effects**, while sample-specific deviations from these fixed effects were modeled as **random effects** to capture the unique desorption characteristics of each individual soil sample.

3.4.3 Comparative Modeling of Soil and Agronomic Parameters

To test the hypotheses of this thesis, two distinct sets of linear mixed-effects models were constructed.

Table 2: Description of variables used in the agronomic and soil models.

Abbreviation	Full.Name	Unit	Description
Y_{rel}	Relative Yield	unitless	Plot yield normalized by the national mean yield for that year and crop.
Y_{norm}	Normalized Yield	unitless	Plot yield normalized by the site-specific median yield of the highest P treatment for that year and crop.
P_{up}	P Uptake	kg P ha ⁻¹	Total P removed by the harvested crop biomass over a growing season.
P_{bal}	P Balance	kg P ha ⁻¹	Net P budget, calculated as P inputs (fertilizer) minus P outputs (uptake).
k	Rate Constant	min ⁻¹	First-order rate constant of P desorption, representing the speed of P release.
P_{desorb}	Desorbable P	mg P L ⁻¹	Maximum desorbable P, representing the size of the readily available P pool.
J_0	Initial P Flux	mg P L ⁻¹ min ⁻¹	Product of k and P_{desorb} , representing the initial flux of P from the soil.
P_{CO2}	Water-Soluble P	mg P kg ⁻¹	Plant-available P measured by CO ₂ -saturated water extraction (Forschungsanstalt für Agrarökologie und Landbau (FAL), 1996).
P_{AAE10}	Chelate-Extractable P	mg P kg ⁻¹	Plant-available P measured by the ammonium-acetate-EDTA extraction method (Forschungsanstalt für Agrarökologie und Landbau (FAL), 1996).
Al_d	Dithionite-Extractable Al	mg Al kg ⁻¹	Free Al oxides (crystalline and amorphous) extracted with dithionite-citrate-bicarbonate (Mehra & Jackson, 1960).
Fe_d	Dithionite-Extractable Fe	mg Fe kg ⁻¹	Free Fe oxides (crystalline and amorphous) extracted with dithionite-citrate-bicarbonate (Mehra & Jackson, 1960).

3.4.4 Model Assumptions and Diagnostics

The validity of the linear mixed-effects models (**lmer**) relies on several key assumptions, primarily that the model residuals are normally distributed and homoscedastic (i.e., have constant variance across the range of predicted values). Prior to finalizing the models, these assumptions were rigorously checked through visual inspection of diagnostic plots, such as quantile-quantile (Q-Q) plots of the residuals and plots of residuals versus fitted values.

Initial exploratory data analysis revealed that several of the predictor variables, most notably the desorbable P pool (P_{desorb} or PS), were strongly right-skewed. Using such variables directly in the linear models would violate the assumptions of linearity and homoscedasticity, leading to potentially biased and unreliable coefficient estimates.

To address this, various transformations (including square root and logarithmic) were tested on the skewed variables. The natural log-transformation ($\log()$) was found to be the most effective at

normalizing the distribution of PS and producing well-behaved model residuals that more closely met the required assumptions. Therefore, $\log(\text{PS})$ was used as a fixed effect in all subsequent agronomic models to ensure the statistical validity of the results.

3.4.4.1 Models of P Availability Metrics as a Function of Soil Properties

First, to investigate the underlying soil-chemical drivers of the different P availability metrics (both kinetic and static), a series of models was built to predict each metric from key soil properties.

- **Fixed Effects Structure:** The fixed effects were identical for all models in this category and included the primary soil physical and chemical properties: clay content, silt content, pH, organic carbon content, and dithionite-extractable iron (Fe_d) and aluminum (Al_d).
- **Random Effects Structure:** The random effects structure accounted for the nested design of the STYCS experiment, with random intercepts for `year`, `Site`, `Site:block`, and `Site:Treatment`.

3.4.4.2 Comparative Models of Agronomic Outcomes

Second, the predictive power of the kinetic parameters was directly compared against that of the standard STP methods (“GRUD” system). For each agronomic response variable (Normalized Yield, P Uptake, and P Balance), two competing models were built. These models shared an identical random effects structure to ensure a fair comparison, differing only in their fixed effects.

- **Random Effects Structure (for all agronomic models):** The structure $(1|\text{year}) + (1|\text{Site}) + (1|\text{Site:block})$ was used to control for variations due to the growing season, location, and in-field spatial differences.
- **Model 1: The Kinetic Approach**
 - **Fixed Effects:** This model used the kinetic parameters and their interaction: $k * \log(\text{PS})$. The interaction term tests the hypothesis that the benefit of a large desorbable P pool (PS) depends on the *rate* (k) at which it can be accessed.
- **Model 2: The Standard STP (GRUD) Approach**
 - **Fixed Effects:** This model used the two standard Swiss soil tests and their interaction: $P_{\text{CO2}} * P_{\text{AAE10}}$.

The relative performance of these two sets of models was then evaluated to determine whether the kinetic parameters provided a significant improvement in predictive power for key agronomic outcomes. Further the relative performance of these two approaches, along with other combinations of predictor sets, was rigorously evaluated using a machine learning benchmark workflow implemented in the `mlr3` package (Lang et al., 2019). The predictive power of each predictor set was quantified using **5-fold cross-validation**. Performance was measured as the percentage of explained variance on the hold-out data $(1 - \text{MSE} / \text{Var}(y))$, providing a robust and unbiased estimate of how well each model would generalize to new data. This benchmark allowed for a direct comparison of the information content provided by the kinetic parameters versus the standard soil tests for predicting key agronomic outcomes.

4 Results

The results of this study are presented in two main parts. First, the development and validation of the phosphorus (P) desorption kinetic model are detailed, justifying the final modeling approach. Second, the descriptive trends of both agronomic outcomes and soil P parameters in response to long-term fertilization and site differences are explored visually. Finally, the predictive power of the kinetic and standard P parameters is formally evaluated using linear mixed-effects models.

4.1 Establishment of the P-Desorption Kinetic Model

The primary goal was to derive two key parameters for each soil sample: the desorbable P pool (P_{desorb}) and the rate constant (k). The analysis proceeded in two stages: an initial test of a linearized model, followed by the implementation of a more robust non-linear model.

4.1.1 Initial Approach: Failure of the Linearized Model

Following the conceptual framework of Flossmann and Richter (1982), the first-order kinetic equation was linearized. A core assumption of this model is that the linear relationship must pass through the origin. To test this, linear models were fitted to the transformed data for each sample individually. The results revealed a systematic failure of this assumption, as the estimated intercepts for the majority of samples were highly significantly different from zero ($p < 0.05$). This consistent statistical deviation indicated that the linearized approach was not a valid representation of the data. The visual evidence in Figure 1 supports this conclusion.

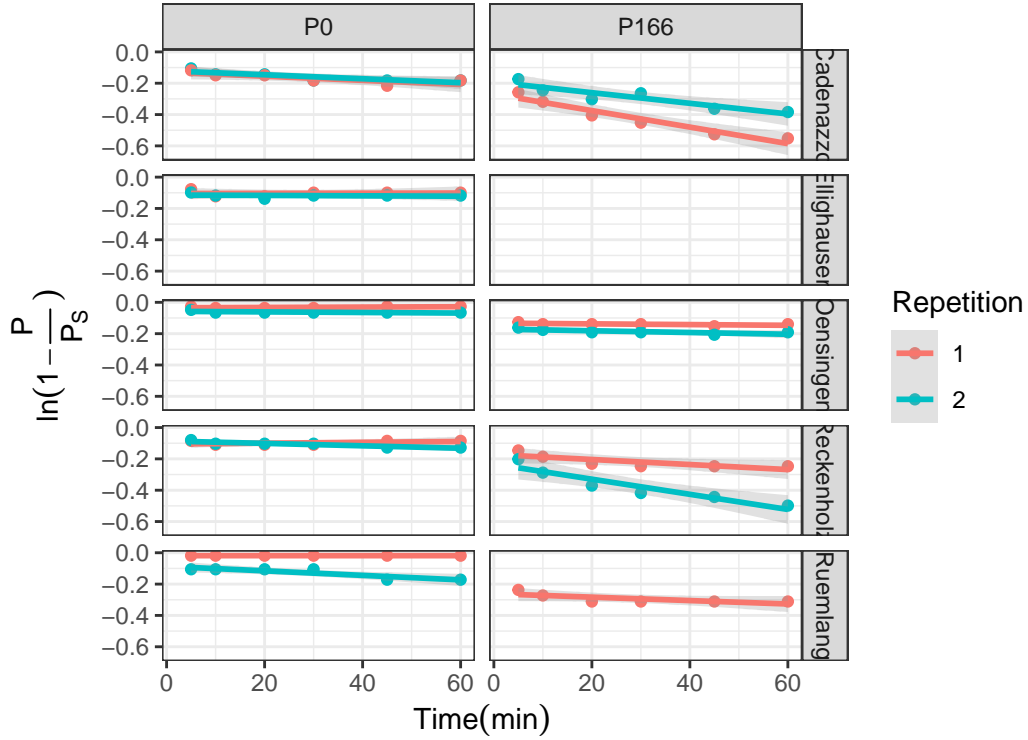


Figure 1: Test of the linearized first-order kinetic model. The plot visually supports the statistical finding that many intercepts are not zero.

4.1.2 Final Approach: Successful Non-Linear Model

Given the statistical failure of the linearized model, a direct non-linear modeling approach was adopted to estimate both P_{desorb} and k simultaneously from the untransformed data. This approach does not rely on the assumption of a zero intercept and proved to be far more successful, accurately capturing the curvilinear shape of the desorption data for nearly all samples (fig-nonlinear-model). The final parameters were extracted from a non-linear mixed-effects model (nlme) to account for the hierarchical data structure. **These final nlme-derived coefficients were used for all subsequent analyses.**

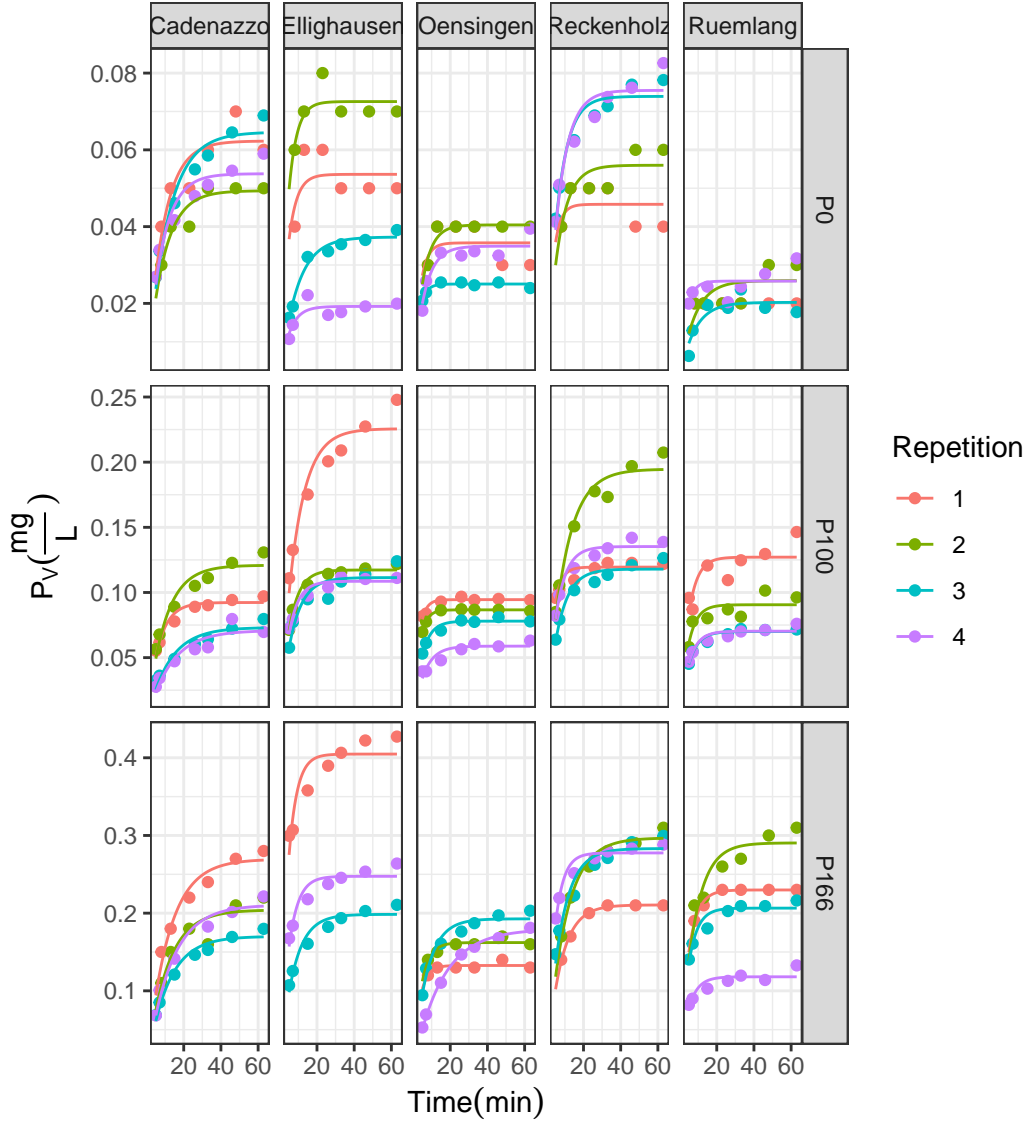


Figure 2: Non-linear first-order kinetic model fits for P desorption over time. Points represent measured data and solid lines represent the fitted model for each replicate.

4.2 Comparison with Isotopic Exchange Kinetics (IEK) {#sec-comparison-with-isotopic-exchange-kinetics-(iek)}

To validate the newly derived kinetic parameters against an established benchmark, the capacity (P_{desorb}) and kinetic (k) parameters were compared to data from Isotopic Exchange Kinetics (IEK) studies previously conducted on the same long-term trial sites by Demaria et al. (2013). This comparison aims to determine if the simpler, non-equilibrium desorption method used in this thesis captures similar aspects of soil P dynamics as the more complex, equilibrium-based IEK method.

The size of the desorbable P pool (P_{desorb}) was compared against the long-term isotopically exchangeable P pool measured after 7 days (E_{7d}). The desorption rate constant (k) was compared against the IEK kinetic parameter measured after 24 hours (n_{1d}). Spearman's rank correlation was used to robustly test for monotonic trends between the different methods.

The analysis revealed a statistically significant, moderate positive correlation between the capacity parameters, P_{desorb} and E_{7d} (fig-iek-comparison). The Spearman's rank correlation coefficient was

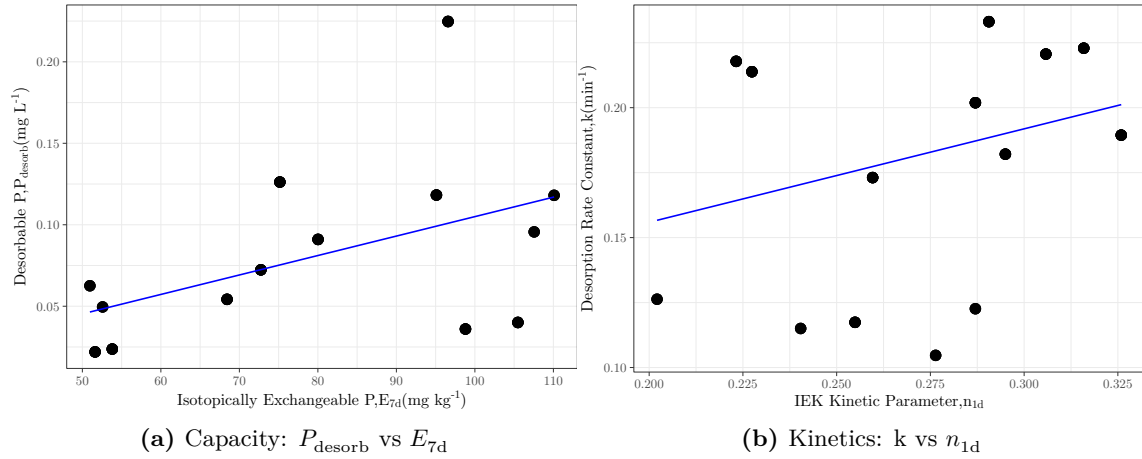


Figure 3: Correlation between desorption-derived kinetic parameters and IEK-derived parameters. (A) Capacity parameters: Desorbable P (P_{desorb}) vs. Isotopically Exchangeable P (E_{7d}). (B) Kinetic parameters: Rate Constant (k) vs. IEK kinetic parameter (n_{1d}).

0.4 with a p-value of < 0.001 .

Similarly, a statistically significant, moderate positive correlation was found between the kinetic parameters, k and n_{1d} (fig-iek-comparison). The Spearman's rank correlation coefficient was 0.36 with a p-value of < 0.001 .

These results indicate that the simpler, non-equilibrium desorption method used in this study successfully captures both the capacity and intensity aspects of soil P lability, providing results that are consistent with the more complex, equilibrium-based IEK method reported by Demaria et al. (2013).

4.3 Effects of Fertilization on Agronomic and Soil Parameters

Having established a robust method to determine the kinetic parameters, the next step was to explore the effects of the long-term P fertilization treatments on both the agronomic outcomes and the soil P test parameters.

4.3.1 Agronomic Responses to P Fertilization

The long-term application of different P fertilization levels had a pronounced impact on the primary agronomic outcomes, including two different metrics for yield, P Uptake (P_{up}), and P Balance (P_{bal}), though the response varied considerably between sites (Figure 4).

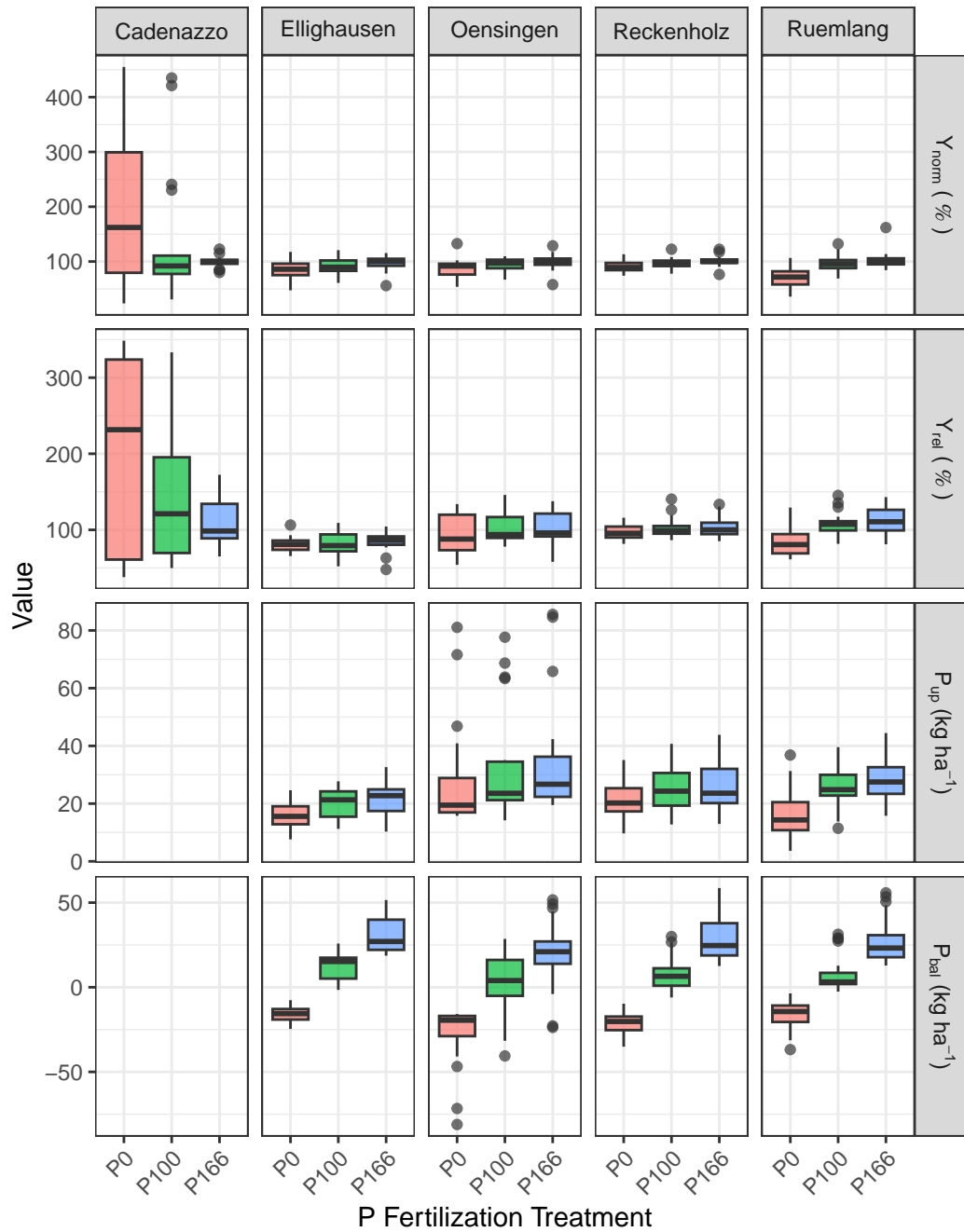


Figure 4: Agronomic response variables across six P fertilization treatments and six experimental sites. Data from 2017-2022.

Yield Metrics (Y_{norm} and Y_{rel}): Both yield metrics showed a generally positive response to P fertilization. The site-normalized yield (Y_{norm}) shows the response relative to the site's potential for that year, with most yields plateauing around the Norm (100%) treatment. The national-normalized yield (Y_{rel}) provides a broader context, showing how yields at each site compare to the national average.

P Uptake (P_{up}): P uptake by crops followed a similar trend to yield, increasing with fertilization, often continuing to increase at the highest fertilization levels, suggesting luxury consumption.

P Balance (P_{bal}): The P balance showed a strong, linear relationship with fertilization. The

Zero and Deficit treatments resulted in a negative balance (mining soil P), while the Elevated and Surplus treatments led to a significant P surplus.

4.3.2 Soil P Parameters as a Function of P Fertilization

The different soil P test parameters, including the standard STP methods and the newly derived kinetic parameters, all responded to the long-term fertilization treatments (Figure 5).

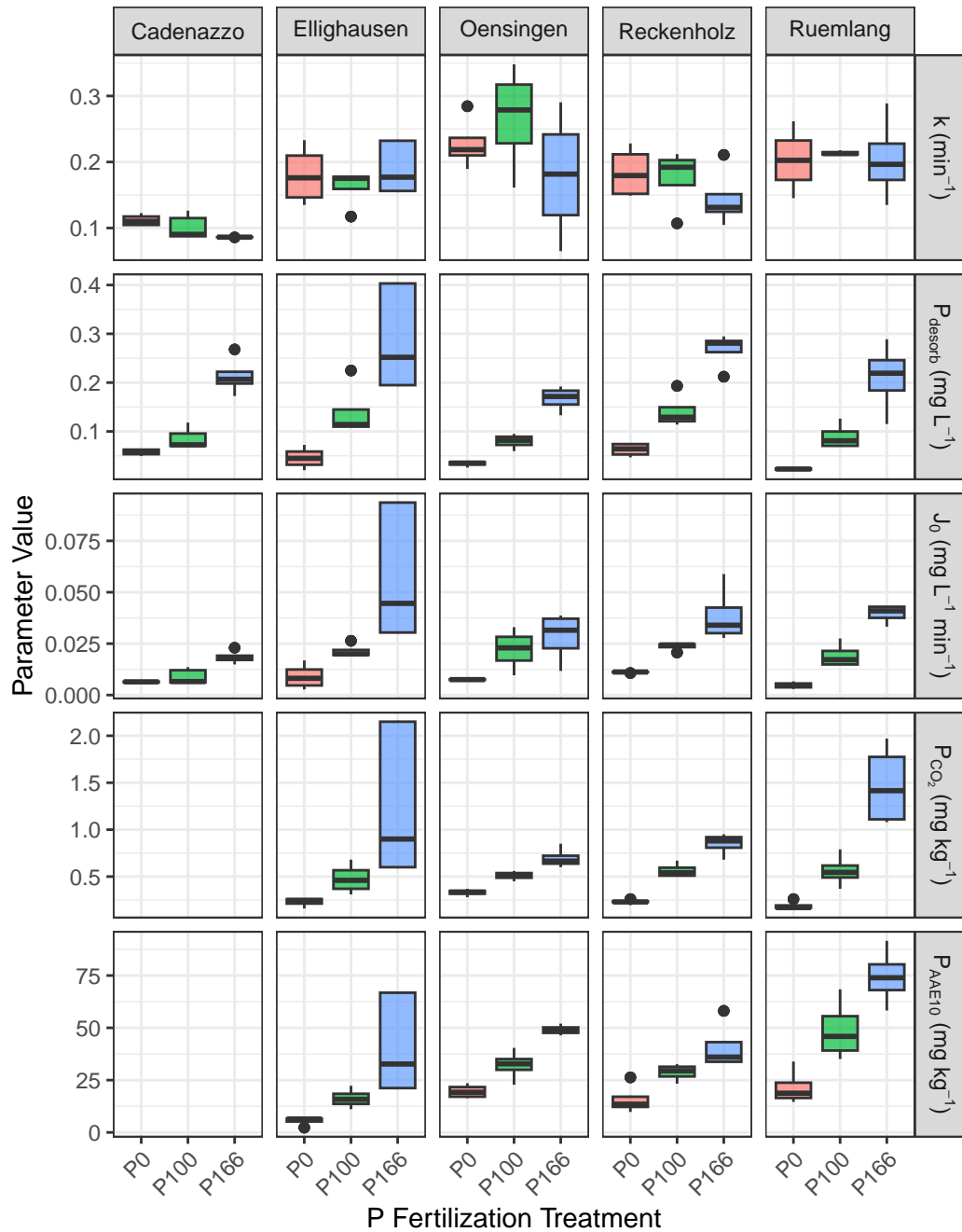


Figure 5: Soil P parameters across six P fertilization treatments and six experimental sites.

Standard STPs (P_{CO_2} and P_{AAE10}): Both standard soil P tests showed a clear and consistent increase with rising P fertilization levels across all sites, confirming their sensitivity to management.

Kinetic Parameters (k , P_{desorb} , and J_0): * **Desorbable P** (P_{desorb}): This parameter behaved very similarly to the standard STPs, increasing steadily with P fertilization and confirming its role as a “capacity” indicator. * **Rate Constant** (k): The rate constant showed a more complex pattern, with no strong, consistent trend with fertilization. This suggests that while fertilization increases the *amount* of available P, it may not change the *intrinsic release rate*. * **Initial P Flux** (J_0): As the product of P_{desorb} and k , this parameter integrates both capacity and intensity. It showed a strong positive response to fertilization, driven primarily by the increase in P_{desorb} .

These initial observations suggest that the kinetic parameters, particularly the rate constant k , may provide unique information about the soil’s P dynamics not captured by static tests alone. The next section will use formal statistical models to test these relationships.

4.4 Predicting P Parameters from Soil Properties

To understand the underlying drivers of the standard and kinetic P parameters, and to test **Hypotheses 1b and 2b**, a series of linear mixed-effects models were fitted. Each model predicted one of the P parameters based on the core soil properties: organic carbon (C_{org}), clay content, silt content, pH, and dithionite-extractable Al (Al_d) and Fe (Fe_d). The results are summarized in Table 3.

Table 3: Results of linear mixed-effects models predicting P parameters from intrinsic soil properties. Significance codes: “ $p < 0.001$, ” $p < 0.01$, ” $p < 0.05$.

Predictor/Model	P_{desorb}	k	J_0	P_{CO_2}	P_{AAE10}
Intercept	21.444	0.454	21.189	14.014	23.126
Al_d	-8.706***	-0.072***	-8.631***	-4.417***	-9.473***
Fe_d	-1.068***	0.005	-1.084***	-0.845***	-0.606***
Clay	-0.006***	-0.016***	-0.085***	0.015	-0.029***
C_{org}	0.612	0.137	1.250	0.269	1.454
pH	-0.018***	-0.021***	-0.092***	0.124	0.012
Silt	-0.000***	0.004	0.008	-0.015***	-0.049***
R_m^2	0.393	0.212	0.368	0.362	0.494
R_c^2	0.996	0.915	0.993	0.995	0.997

The analysis reveals that the capacity-based P pools and the kinetic rate constant are controlled by different sets of soil properties, strongly supporting the hypotheses.

In line with **Hypothesis 2b**, the kinetic capacity parameter, **Desorbable P** (P_{desorb}), showed a highly significant negative relationship with both dithionite-extractable iron (Fe_d) and aluminum (Al_d). This provides strong evidence that the total pool of free oxides, which represent the primary P sorption surfaces in the soil, is a key factor controlling the size of the readily desorbable P pool.

Also confirming **Hypothesis 2b**, the **Rate Constant** (k) was governed by a different set of properties. It was not significantly influenced by the free oxides but instead showed a significant negative relationship with **Clay** content and a positive relationship with organic carbon (C_{org}). This clearly distinguishes the kinetic component from the capacity component, suggesting that while oxides control *how much* P can be held, soil texture and organic matter influence *how fast* it can be released.

The standard STP methods showed patterns consistent with **Hypothesis 1b**. **Organic Carbon** (C_{org}) had a highly significant positive effect on P_{AAE10} , and **pH** had a significant negative effect, as predicted. The relationship of the STP measures with the dithionite-extractable oxides was less consistent than that of P_{desorb} , with only P_{AAE10} showing a significant negative link to Al_d .

4.5 Predictive Modeling of Agronomic Outcomes

To formally evaluate the predictive power of the standard STP methods against the kinetic parameters, a series of linear mixed-effects models were fitted for each of the primary agronomic response variables. To test the central hypotheses of this thesis, the predictive power of the kinetic parameters was directly compared against that of the standard STP methods for several key agronomic outcomes. For each response variable—Normalized Yield (Y_{rel}), P Uptake (P_{up}), and P Balance (P_{bal})—a set of competing linear mixed-effects models was constructed.

To ensure a fair comparison, all models shared an identical random effects structure ((1|year) + (1|Site) + (1|Site:block)), differing only in their fixed effects. Four distinct models were evaluated: * P_{CO_2} **Model:** Used the standard water-soluble P test as the sole predictor. * P_{AAE10} **Model:** Used the standard chelate-extractable P test as the sole predictor. * **STP Interaction Model:** Included both standard tests and their interaction term ($P_{CO_2} * P_{AAE10}$) to capture their combined effect. * **Kinetic Model:** Used the log-transformed desorbable P pool ($\log(P_{desorb})$), the rate constant (k), and their interaction (J_0) as predictors.

The performance of these models for each agronomic outcome is presented in the following sections.

4.5.1 Predicting Site-Normalized Yield (Y_{norm})

When predicting yield normalized to the site's own potential, the standard STP methods, particularly P_{CO_2} , were the most effective predictors (Table 4). The model including both STP methods ($P_{CO_2} * P_{AAE10}$) achieved a marginal R^2 of 0.22, explaining a substantial portion of the variance in within-site yield response. The kinetic model also performed well, explaining 16.5% of the variance (marginal $R^2 = 0.165$), with the desorbable P pool (P_{desorb}) being a highly significant predictor. This indicates that for optimizing yield within a given field, both static and kinetic capacity measures are effective.

Table 4: Results of linear mixed-effects models predicting Site-Normalized Yield (Y_{norm}).

Predictor/Model	P_{CO_2}	STP- Interaction	kinetic	
Intercept	1.059***	0.532***	1.096***	0.980
k				2.262
J_0				0.931
P_{desorb}				-0.063
P_{AAE10}		0.120***	-0.006	
P_{CO_2}	0.162***		0.137	
$P_{CO_2} \times P_{AAE10}$			0.016	
R_m^2	0.218	0.198	0.220	0.014
R_c^2	0.358	0.474	0.365	0.360

The analysis reveals a clear and striking difference between the predictive power of the standard STP methods and the kinetic parameters for site-normalized yield.

The standard STP methods were highly effective predictors. Both the P_{CO_2} and P_{AAE10} models showed highly significant coefficients and explained a substantial portion of the variance, with marginal R^2 values of 0.218 and 0.198, respectively. The combined model (STP-interaction) performed best overall, explaining 22% of the variance fixed effects. These results directly contradict **Hypothesis 1a**, which posited that these static measurements would be weak predictors of yield. For predicting yield relative to a site's own maximum potential, the standard soil tests perform very well.

In stark contrast, the kinetic model had virtually no predictive power for Y_{norm} . The model's marginal R^2 was only 0.014, and none of the kinetic parameters—neither the rate constant (k), the

desorbable pool (P_{desorb}), nor their interaction—were statistically significant. This finding strongly refutes **Hypothesis 3** for this specific yield metric. The results suggest that when agronomic potential is evaluated within a single site (the function of site-normalization), the rate of P supply is not the limiting factor; rather, the overall capacity or size of the available P pool, as measured effectively by standard soil tests, is the dominant driver of the yield response.

4.5.2 Predicting National-Normalized Yield (Y_{rel})

The models predicting national-normalized yield (Y_{rel}) reveal that both standard and kinetic soil phosphorus tests struggle to explain the variance in crop yields on their own, though standard tests show slightly better performance in this context.

Table 5: Results of linear mixed-effects models predicting National-Normalized Yield (Y_{rel}).

Predictor/Model	P_{CO_2}	P_{AAE10}	STP-interaction	kinetic
Intercept	104.862***	75.343***	130.274***	56.375
k				377.498**
J_0				171.507**
P_{desorb}				-27.486*
P_{AAE10}		7.111**	-6.537	
P_{CO_2}	8.853**		23.091	
$P_{CO_2} \times P_{AAE10}$			-3.110	
R_m^2	0.074	0.063	0.078	0.022
R_c^2	0.569	0.537	0.596	0.439

4.5.2.1 Performance of Standard STP Methods

The models based on standard soil tests (P_{CO_2} and P_{AAE10}) individually showed a significant, positive relationship with relative yield. When considered alone, both P_{CO_2} and P_{AAE10} were significant predictors, explaining 7.4% and 6.3% of the variance in yield, respectively (indicated by their marginal R^2 , R_m^2). The model including their interaction term ($P_{CO_2} * P_{AAE10}$) performed slightly better, explaining 7.8% of the variance.

These findings partially align with **Hypothesis 1a**, which posited that standard STP methods would be weak predictors of relative crop yield. The low marginal R^2 values confirm that these static measurements account for less than 8% of the yield variation, which is indeed a weak predictive performance.

4.5.2.2 Performance of the Kinetic Model

Contrary to expectations, the model based on kinetic parameters ($k * P_{desorb}$) demonstrated very low predictive power, with a marginal R^2 of just 2.2%. Although the desorption rate (k) and the initial P flux (J_0) showed a significant positive relationship with yield, the overall model performed worse than the standard STP methods.

This result directly contradicts **Hypothesis 3**, which stated that a model incorporating kinetic parameters would explain a significantly greater proportion of the variance in relative yield compared to static STP measurements. For predicting national-normalized yield, the opposite appears to be true; the standard methods, while weak, still outperform the kinetic approach.

4.5.2.3 The Role of Unmeasured Factors

A critical observation across all models is the large discrepancy between the marginal R^2 (R_m^2) and the conditional R^2 (R_c^2). The conditional R^2 represents the total variance explained by both the fixed effects (the predictors like P_{CO_2} or k) and the random effects (such as **Site** and **year**).

For instance, in the best-performing STP model (STP-interaction), the marginal R^2 is only 0.078, but the conditional R^2 is 0.596. This means that while the soil P measurements themselves explain about 8% of the yield variance, the combination of soil tests *plus* the site- and year-specific conditions explains nearly 60% of it. This pattern holds for all models and strongly suggests that pedoclimatic factors, captured by the **Site** and **year** random effects, are the dominant drivers of crop yield in this dataset, overshadowing the influence of the measured soil P parameters.

4.5.3 Predicting P-Uptake (P_{up})

When predicting P-uptake, both the standard and kinetic models demonstrate similarly weak predictive power, with none of the approaches standing out as superior.

Table 6: Results of linear mixed-effects models predicting P-Export (P_{up}).

Predictor/Model	P_{CO_2}	P_{AAE10}	STP-interaction	kinetic
Intercept	27.522***	8.090	30.632*	29.599***
k				22.622
J_0				11.928
P_{desorb}				1.954
P_{AAE10}		4.824***	-0.805	
P_{CO_2}	5.177***		8.069	
$P_{CO_2} \times P_{AAE10}$			-0.814	
R_m^2	0.064	0.073	0.065	0.064
R_c^2	0.625	0.603	0.623	0.648

4.5.3.1 Performance of Standard STP Methods

The standard soil tests, P_{CO_2} and P_{AAE10} , when modeled individually, were significant positive predictors of P-uptake. The P_{AAE10} model performed slightly better, explaining 7.3% of the variance ($R_m^2 = 0.073$) compared to the P_{CO_2} model's 6.4% ($R_m^2 = 0.064$). Interestingly, the interaction model did not improve but slightly decreased the explained variance ($R_m^2 = 0.065$), and the individual predictors lost their significance.

These results are consistent with **Hypothesis 1a**, which predicted that standard STP methods would be weak predictors of agronomic outcomes like P-uptake. The low marginal R^2 values confirm that these static tests, while statistically significant on their own, account for a very small fraction of the variability in P-uptake by crops.

4.5.3.2 Performance of the Kinetic Model

The kinetic model performed on par with the standard individual tests, explaining 6.4% of the variance in P-uptake ($R_m^2 = 0.064$). However, none of the kinetic parameters (k , P_{desorb} , or J_0) emerged as individually significant predictors.

This finding challenges **Hypothesis 3**, which anticipated that the kinetic parameters would offer significantly improved predictive power. For P-uptake, the kinetic model shows no advantage over the simpler, traditional STP methods. The dynamic measures of P supply do not appear to capture the mechanisms driving P-uptake any better than the static measures in this context.

4.5.3.3 Dominance of Site and Year Effects

As with the yield predictions, there is a vast difference between the marginal R^2 and conditional R^2 values across all P-uptake models. For example, the kinetic model's marginal R^2 is only 0.064, but its conditional R^2 is 0.648. This indicates that the fixed effects (the soil P measurements) explain about 6% of the variance, while the random effects (**Site** and **year**) account for the vast majority

of the explained variance (around 58%). This again underscores that site-specific pedoclimatic conditions and year-to-year environmental variations are the primary factors controlling P-uptake, with the specific soil P status playing a minor, secondary role

4.5.4 Predicting P-Balance (P_{bal})

The prediction of the P-Balance (P_{bal}) reveals a stark and decisive contrast between the kinetic and standard STP approaches, providing the strongest evidence in favor of the kinetic methodology.

Table 7: Results of linear mixed-effects models predicting P-Balance (P_{bal}).

Predictor/Model	P_{CO_2}	P_{AAE10}	STP-interaction	kinetic
Intercept	4.441	7.691	3.649	43.833***
k				84.993
J_0				33.029
P_{desorb}				16.947***
P_{AAE10}		-0.794	0.187	
P_{CO_2}	-0.928		-2.442	
$P_{CO_2} \times P_{AAE10}$			0.462	
R_m^2	0.001	0.001	0.001	0.572
R_c^2	0.810	0.807	0.811	0.744

4.5.4.1 Performance of the Kinetic Model

The kinetic model emerged as an exceptionally strong predictor of the P-Balance, explaining 57.2% of the variance ($R_m^2 = 0.572$). The desorbable P pool (P_{desorb}) was a highly significant predictor ($p < 0.001$). This result provides powerful support for the underlying premise of this thesis. The P-Balance represents the net result of P inputs and outputs over time, and the fact that P_{desorb} —a measure of the readily available P pool—so accurately reflects this balance is a significant finding.

This strongly supports **Hypothesis 3**, which asserted that kinetic parameters would be more effective predictors than static tests. In the case of P-Balance, the kinetic model is not just an improvement; it is the only effective model.

4.5.4.2 Performance of Standard STP Methods

In stark contrast, all models based on the standard STP methods (P_{CO_2} , P_{AAE10} , and their interaction) completely failed to predict the P-Balance. Their marginal R^2 values were effectively zero ($R_m^2 = 0.001$), indicating they have no predictive power whatsoever for this crucial agronomic metric. None of the STP predictors were statistically significant.

This finding directly contradicts **Hypothesis 1a**, which anticipated a significant correlation between the standard STP methods and the P-Balance. The results show no such relationship exists, suggesting that these static measurements do not adequately reflect the long-term phosphorus status of the soil as represented by the P-Balance.

4.5.4.3 Interpreting the R^2 Discrepancy

The dramatic difference in performance is clear from the R^2 values. While the conditional R^2 for the STP models is high (around 0.81), their marginal R^2 is 0.001. This indicates that all the explanatory power comes from the random effects (**Site** and **year**), and the STP measurements themselves contribute nothing. The kinetic model, however, has both a high marginal R^2 (0.572) and a high conditional R^2 (0.744). This demonstrates that the kinetic parameters are themselves powerful predictors, capturing a large portion of the variance that is independent of site and year effects.

5 Discussion

This study aimed to determine if dynamic P desorption parameters could provide a more accurate prediction of agronomic outcomes than traditional static soil tests. The results reveal a complex story: the ideal P testing method is not universal but is instead contingent on the specific question being addressed, whether it is optimizing yield within a single field, comparing productivity across different regions, or managing long-term nutrient budgets.

5.1 Hypothesis 1: The Nuanced Role of Standard Soil Tests

Hypothesis 1a posited that standard STP methods (P_{CO_2} and P_{AAE10}) would correlate with the P-Balance but be weak predictors of crop yield. The findings challenge this hypothesis in two unexpected ways.

First, the STP methods **failed completely to predict the P-Balance**. The models showed no relationship between these static tests and the long-term nutrient surplus or deficit, directly contradicting our hypothesis. This is a critical finding, as it suggests that while tests like P_{CO_2} and P_{AAE10} are sensitive to short-term changes from annual fertilization, they do not adequately capture the cumulative, long-term P status of the soil system.

Second, the performance of STP methods in predicting yield was highly context-dependent. When predicting **site-normalized yield** (Y_{norm}), which assesses the yield response relative to a site's own potential, the STP models were remarkably effective, explaining up to 22% of the variance. This result contradicts the part of our hypothesis that expected weak performance and suggests that for *within-field* management, where the goal is to ensure P is not limiting relative to that specific environment's potential, traditional capacity-based tests are well-suited and robust.

However, when predicting **national-normalized yield** (Y_{rel}) and **P-uptake** (P_{up}), the STP models performed poorly, aligning with our initial expectations. The weak performance in predicting yield and P-uptake can likely be attributed to several factors. Firstly, crop yield in field settings is often co-limited by multiple factors beyond phosphorus. Year-to-year variations in climate, such as solar radiation and water availability, as well as the supply of other key nutrients like nitrogen, can become the primary drivers of productivity, masking the more subtle influence of soil P status (Sadras, 2002; Sinclair, 1998). The large gap between the marginal and conditional R^2 in our models strongly suggests that these site- and year-specific variables, captured by the random effects, were indeed the dominant factors.

Furthermore, response variables like P_{up} and P_{bal} are calculated as the product of yield and P concentration, which can introduce and propagate measurement uncertainty. If yield itself is only weakly correlated with soil P status, this “noise” is carried into the derived variables, making it even more difficult to establish a clear statistical relationship (Rowe et al., 2016).

The predictive weakness may also stem from the experimental design and modeling approach. This study utilized samples primarily from the P-deficient (0%) and P-sufficient (100% and 167%) treatments. Crop yield response to fertilizer typically follows a saturation curve, and it is possible that our dataset was concentrated on the less responsive parts of this curve, thus lacking statistical power in the most dynamic range (Schlesinger, 2009). While our use of a linear mixed-effects model was appropriate for the available data, it cannot capture the diminishing returns characteristic of crop nutrient response. As demonstrated by **Hirte et al. (2021)** on these same STYCS trials, non-linear models like the Mitscherlich equation are better suited for describing such saturation kinetics but would require data from the intermediate fertilization levels to be applied robustly (Hirte, Stüssel, et al., 2021).

Regarding **Hypothesis 1b**, the findings were largely supportive. The analysis of soil properties confirmed that STP measurements are not pure measures of P but are instead complex indices reflecting a combination of P status and overarching soil chemistry. The predicted negative relationship between **pH** and P_{AAE10} was observed, and the underlying chemical mechanisms for

this are well-established, particularly in calcareous or high-pH soils like several in this study (e.g., ALT, GRA).

The AAE10 method relies on two key components: ammonium acetate as a buffer and EDTA as a chelating agent to dissolve mineral-bound P. However, its effectiveness is compromised in soils with high pH and an abundance of free calcium (Ca^{2+}) and magnesium (Mg^{2+}) cations, often from calcium carbonates ($CaCO_3$). There are two primary reasons for this:

1. **Consumption of EDTA:** The primary role of EDTA is to bind to cations like iron and aluminum that precipitate phosphate, thereby releasing P into the solution. However, EDTA has a high affinity for divalent cations, so in calcareous soils, a significant portion of the EDTA is consumed by binding to the abundant free Ca^{2+} and Mg^{2+} , making it less available to extract the target phosphate compounds (Fixen & Grove, 1993).
2. **Buffering Capacity:** The acetate buffer in the AAE10 solution is designed to maintain a consistent pH. However, soils with high carbonate content have a strong natural buffering capacity that can resist the pH change intended by the extractant, further reducing its efficiency in dissolving pH-sensitive P minerals.

This known limitation explains why P_{AAE10} can underestimate plant-available P in calcareous soils and supports our finding of a significant pH-dependence. It underscores that the choice of an appropriate soil test must take into account the fundamental chemistry of the soil matrix itself.

5.2 Hypothesis 2: Characterizing P Desorption Kinetics

Hypothesis 2a focused on the methodological feasibility of characterizing P desorption. It predicted that while the process would follow first-order kinetics, a non-linear modeling approach would be more robust than the original linearized method proposed by Flossmann & Richter (1982). The results from this thesis unequivocally support this hypothesis. Our initial attempts to linearize the desorption data failed systematically, with model intercepts deviating significantly from the required origin, thus violating a core assumption of the method. In contrast, the direct application of a non-linear mixed-effects model successfully captured the curvilinear nature of P release for nearly all samples. This confirms that while the foundational concept of first-order kinetics is sound, modern computational methods that avoid data transformation provide a far more accurate and statistically valid approach to parameter estimation (Kuang et al., 2012).

While the non-linear model proved robust, visual inspection of the kinetic curves revealed that two specific replicates—from the P100 and P166 treatments at the Ellighausen site—showed markedly higher and faster P release than their counterparts. To determine whether this was due to a methodological artifact or true field variability, the standard soil test results for all replicates at this site were examined (Figure 6). The diagnostic plot clearly shows that these same two replicates also registered as significant outliers for both P_{CO_2} and P_{AAE10} . This consistent pattern across three independent measurement techniques strongly suggests that the deviation is not a result of error in the kinetic procedure, but rather reflects genuine **micro-site heterogeneity**.

Such heterogeneity could arise from several sources. One plausible explanation, given the decades-long application of Triple-Superphosphate (primarily monocalcium phosphate), is the presence of residual, undissolved fertilizer granules in the soil matrix. The accidental inclusion of even a single such particle in the 10g subsample for a specific replicate would lead to artificially inflated P values across all chemical extractions. This highlights a fundamental challenge in soil analysis and reinforces the importance of robust modeling. The use of a non-linear *mixed-effects* model is particularly advantageous in this context, as it is designed to handle such individual variations by estimating a common overall trend while allowing for random deviations for each sample, thereby preventing a few anomalous data points from unduly influencing the overall conclusions [Fisher (1925); Fisher 1935; Yates 1964; Van Es et al. (2002)].

Ultimately, the successful validation of our derived parameters against established Isotopic Exchange Kinetic (IEK) data further solidifies the robustness of our methodological approach, demonstrating

that this simpler extraction method effectively captures both the capacity (P_{desorb}) and intensity (k) aspects of P dynamics.

```
# Make sure the required libraries are loaded
library(ggplot2)
library(dplyr)

# Filter for the Ellighausen site and select relevant columns
ell_data <- D %>%
  filter(Site == "Ellighausen") %>%
  select(Treatment, Rep, soil_0_20_P_CO2, soil_0_20_P_AAE10)

# Determine the scaling factor for the secondary axis.
# This is a common approach: divide the range of the primary variable by the range of the secondary
scaling_factor <- max(ell_data$soil_0_20_P_AAE10, na.rm = TRUE) / max(ell_data$soil_0_20_P_CO2, na.rm = TRUE)

# Create the plot
ggplot(ell_data, aes(x = as.factor(Rep), group = 1)) +
  # Plot the first variable (P_AAE10) - this will use the primary (left) y-axis
  geom_line(aes(y = soil_0_20_P_AAE10, color = "blue")) +
  geom_point(aes(y = soil_0_20_P_AAE10, color = "blue", size = 4)) +

  # Plot the second variable (P_CO2) - transform it by the scaling factor
  geom_line(aes(y = soil_0_20_P_CO2 * scaling_factor, color = "red")) +
  geom_point(aes(y = soil_0_20_P_CO2 * scaling_factor, color = "red", size = 4)) +

  # Create the secondary y-axis
  scale_y_continuous(
    # Features for the primary y-axis
    name = "P_AAE10 (mg/kg)",

    # Add the secondary y-axis and define its properties
    sec.axis = sec_axis(
      # The transformation here is the INVERSE of the one we applied to the data
      trans = ~ . / scaling_factor,
      name = "P_CO2 (mg/kg)"
    )
  ) +
  facet_wrap(~ Treatment, scales = "free_y") +
  labs(
    title = "Standard Soil P Tests at Ellighausen",
    x = "Replicate Number",
    y = "P Concentration (mg/kg)" # This label is now redundant but kept for convention
  ) +
  theme_bw() +
  # Adjust colors for the axis titles and text to match the lines
  theme(
    axis.title.y.left = element_text(color = "blue"),
    axis.text.y.left = element_text(color = "blue"),
    axis.title.y.right = element_text(color = "red"),
    axis.text.y.right = element_text(color = "red")
  )
```

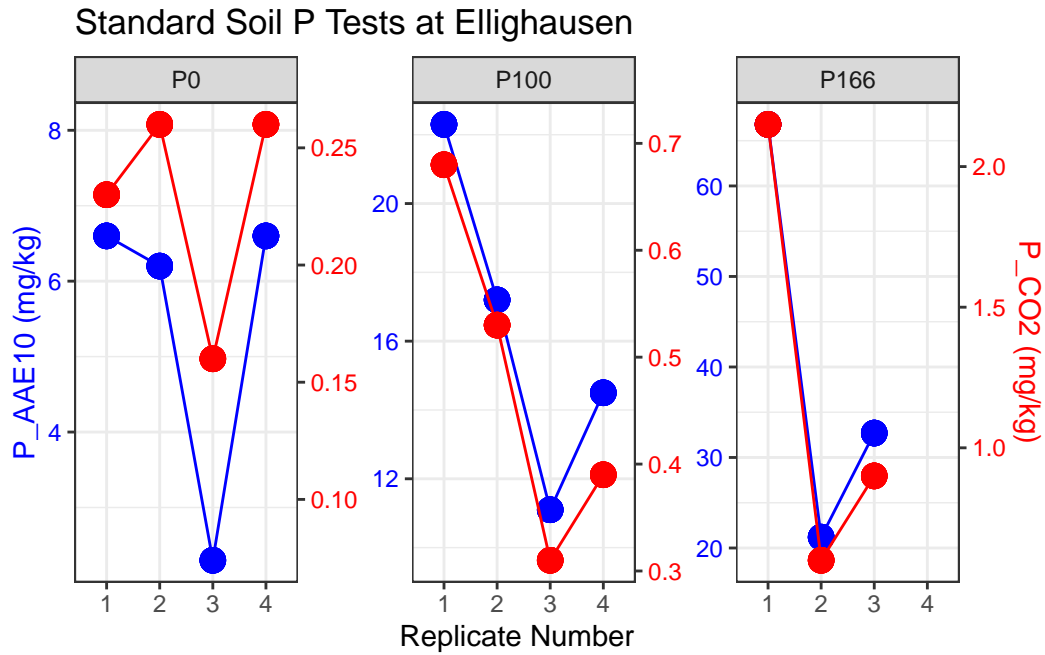


Figure 6: Diagnostic plot for P_AAE10 (left axis) and P_CO2 (right axis) for all replicates at the Ellighausen (ELL) site, faceted by P fertilization treatment.

Hypothesis 2b predicted that the derived kinetic parameters would be significantly influenced by fundamental soil properties, and this was also strongly supported by the findings. The analysis revealed a clear and meaningful separation in the drivers of the capacity and kinetic components. The desorbable P pool (P_{desorb}), representing the quantity of readily available P, was strongly and negatively correlated with dithionite-extractable iron and aluminum. This aligns perfectly with established soil science principles, as these free oxides provide the primary sorption surfaces that bind P, thereby controlling the size of the exchangeable pool (Brady & Weil, 2016; Sposito, 2008).

Conversely, the rate constant (k), which represents the speed of P release, was not primarily driven by the oxide content but was instead significantly related to soil texture (clay content) and pH. The negative relationship with clay content is logical, as higher clay content can increase the tortuosity of diffusion pathways, effectively slowing the movement of phosphate from the solid phase to the bulk solution (Nye & Tinker, 2000). The influence of pH is also consistent with known phosphate chemistry, as pH governs the speciation of orthophosphate ions and their affinity for mineral surfaces (Sparks, 2003). These distinct relationships confirm that P_{desorb} and k are not redundant parameters; they represent fundamentally different aspects of P availability—the size of the pool and the rate of access to it—which are governed by different soil-chemical and physical properties.

6 Conclusion

7 Acknowledgments

8 Legal Disclosure

9 References

- Abelson, P. H. (1999). The global phosphorus dilemma: A new insight into an old problem. *Science*, 283(5410), 2015. <https://doi.org/10.1126/science.283.5410.2015>
- Bates, D., Mächler, M., Bolker, B., & Walker, S. (2015). Fitting linear mixed-effects models using lme4. *Journal of Statistical Software*, 67(1), 1–48. <https://doi.org/10.18637/jss.v067.i01>
- Bell, R. W., Bell, M. J., & M. Tavora, W. J. G. de. (2013). Factors influencing the soil test calibration for colwell p and wheat under winter-dominant rainfall. *Crop and Pasture Science*, 64(5), 489–501. <https://doi.org/10.1071/CP13019>
- Berg, J. M., Tymoczko, J. L., Jr., G. J. G., & Stryer, L. (2019). *Biochemistry* (9th ed.). W. H. Freeman; Company.
- Bohn, H. L., Myer, R. A., & O'Connor, G. A. (2002). *Soil and water chemistry: An integrative approach* (3rd ed.). John Wiley & Sons.
- Brady, N. C., & Weil, R. R. (2016). *The nature and properties of soils* (15th ed.). Pearson.
- Fardeau, J. C., Morel, C., & Boniface, R. (1991). Phosphate ion transfer from soil to soil solution: Kinetic parameters. *Agronomie*, 11(9), 787–797. <https://doi.org/10.1051/agro:19910908>
- Fisher, R. A. (1925). *Statistical methods for research workers*. Oliver; Boyd.
- Fixen, P. E., & Grove, J. H. (1993). Testing soils for phosphorus. *Soil Science Society of America Book Series*, 3, 141–180. <https://doi.org/10.2136/sssabookser3.2ed.c11>
- Flossmann, R., & Richter, D. (1982). *Extraction method for characterizing the kinetics of phosphorus release from solid soil to soil solution*.
- Forschungsanstalt für Agrarökologie und Landbau (FAL). (1996). *Methodenbuch für boden-, pflanzen- und nährstoffanalysen*. FAL.
- Frossard, E., Condron, L. M., Oberson, A., Sinaj, S., & Fardeau, J. C. (2000). Processes governing phosphorus availability in temperate soils. *Journal of Environmental Quality*, 29(1), 15–23. <https://doi.org/10.2134/jeq2000.00472425002900010003x>
- Gerke, J. (2010). Humic (organic matter)-al(fe)-phosphate complexes: An underestimated phosphate form in soils and source of plant-available phosphate. *Soil Science*, 175(9), 417–425. <https://doi.org/10.1097/SS.0b013e3181f26a1d>
- Hinsinger, P. (2001). Phosphorus dynamics in the soil-plant continuum: A review. *Plant and Soil*, 237(2), 167–191. <https://doi.org/10.1023/A:1013339317511>
- Hirte, J., Leifeld, J., Laggoun-Défarge, A., Mayer, P., & Gubler, J. M. (2018). Relationship between soil phosphorus, phosphorus budget, and soil properties in swiss agricultural soils. *Ambio*, 47(Suppl 1), 53–64. <https://doi.org/10.1007/s13280-017-0987-9>
- Hirte, J., Richner, W., Orth, B., Liebisch, F., & Flisch, R. (2021). Yield response to soil test phosphorus in Switzerland: Pedoclimatic drivers of critical concentrations for optimal crop yields using multilevel modelling. *Science of The Total Environment*, 755, 143453. <https://doi.org/10.1016/j.scitotenv.2020.143453>
- Hirte, J., Stüssel, C. E. M., Leifeld, J., Gubler, J. M., Sinaj, S., & Frossard, E. (2021). Yield response to soil test phosphorus in switzerland: Pedoclimatic drivers of critical concentrations for optimal crop yields using multilevel modelling. *Agriculture, Ecosystems & Environment*, 309, 107270. <https://doi.org/10.1016/j.agee.2020.107270>
- Holford, I. C. R. (1997). Soil phosphorus: Its measurement, and its uptake by plants. *Australian Journal of Soil Research*, 35(2), 227–239. <https://doi.org/10.1071/S96047>
- Johnston, A. E., Poulton, P. R., & Goulding, K. W. T. (2001). Phosphorus in soils, crop production and water quality. *The Scientific World Journal*, 1, 304–311. <https://doi.org/10.1100/tsw.2001.272>
- Kuang, W., Wang, W. J., Liu, X. J., Cui, Y. F., Chen, Z. H., Wang, B. R., & Lin, X. Y. (2012). Phosphorus desorption kinetics in soils with different long-term fertilization: A comparison of kinetic models. *Journal of Soils and Sediments*, 12, 739–749. <https://doi.org/10.1007/s11368-012-0498-8>
- Kuznetsova, A., Brockhoff, P. B., & Christensen, R. H. B. (2017). lmerTest package: Tests in linear mixed effects models. *Journal of Statistical Software*, 82(13), 1–26. <https://doi.org/10.18637/jss.v082.i13>
- Lang, M., Binder, M., Richter, J., Schratz, P., Casalicchio, G., Coors, S., Pfisterer, F., Fischer, S.,

- Au, Q., & Bischl, B. (2019). mlr3: A modern object-oriented machine learning framework in R. *Journal of Open Source Software*, 4(44), 1903. <https://doi.org/10.21105/joss.01903>
- McDowell, R. W., & Sharpley, A. N. (2001). Approximating phosphorus release from soils to surface runoff and subsurface drainage. *Journal of Environmental Quality*, 30(2), 508–520. <https://doi.org/10.2134/jeq2001.302508x>
- Mehra, O. P., & Jackson, M. L. (1960). Iron oxide removal from soils and clays by a dithionite-citrate system buffered with sodium bicarbonate. *Clays and Clay Minerals*, 7, 317–327.
- National Institutes of Health, Office of Dietary Supplements. (2023). *Phosphorus: Fact sheet for health professionals*. <https://ods.od.nih.gov/factsheets/Phosphorus-HealthProfessional/>
- Nelson, D. L., Cox, M. M., & Hoskins, A. A. (2021). *Lehninger principles of biochemistry* (8th ed.). Macmillan Learning.
- Nye, P. H., & Tinker, P. B. (2000). *Solute movement in the rhizosphere*. Oxford University Press.
- Pinheiro, J., Bates, D., DebRoy, S., Sarkar, D., & R Core Team. (2022). *Nlme: Linear and nonlinear mixed effects models*. <https://CRAN.R-project.org/package=nlme>
- R Core Team. (2022). *R: A language and environment for statistical computing*. R Foundation for Statistical Computing. <https://www.R-project.org/>
- Rast, W., & Thornton, J. A. (1996). A eutrophication of waters: Control and management. In G. E. Likens (Ed.), *Limnology and oceanography* (pp. 253–289). Chapman & Hall.
- Rowe, H., Withers, P. J. A., Baas, P., Chan, N. I., Doody, D., Holiman, J., Jacobs, B., Li, H., MacDonald, G. K., McDowell, R., Sharpley, A. N., Shen, J., Salm, C. van der, & Weigelt, A. (2016). Integrating legacy phosphorus into sustainable nutrient management strategies for future food, bioenergy and water security. *Nutrient Cycling in Agroecosystems*, 104(3), 393–412. <https://doi.org/10.1007/s10705-015-9726-1>
- Sadras, V. O. (2002). Co-limitation of crop yield by water and nitrogen in semi-arid environments. *Agronomie*, 22(5), 433–445. <https://doi.org/10.1051/agro:2002018>
- Schlesinger, W. H. (2009). *Biogeochemistry: An analysis of global change* (2nd ed.). Academic Press.
- Schofield, R. K. (1955). Can a precise meaning be given to 'available' soil phosphorus? *Soils and Fertilizers*, 18, 373–375.
- Sharpley, A. N., Daniel, T. C., Sims, J. T., Lemunyon, J. L., Stevens, R. G., & Parry, R. W. (2000). Agricultural phosphorus and eutrophication. *Journal of Environmental Quality*, 29(1), 1–9. <https://doi.org/10.2134/jeq2000.00472425002900010001x>
- Sharpley, A. N., Duiker, S. W., & Feyereisen, G. W. (2003). Improving the agricultural water quality in the u.s. *Journal of Environmental Quality*, 32(2), 421–439. <https://doi.org/10.2134/jeq2003.4210>
- Sims, J. T., & Sharpley, A. N. (Eds.). (2005). *Phosphorus: Agriculture and the environment*. American Society of Agronomy, Crop Science Society of America, Soil Science Society of America. <https://doi.org/10.2134/agronmonogr46>
- Sinclair, T. R. (1998). Historical changes in harvest index and crop nitrogen accumulation. *Crop Science*, 38(3), 638–643. <https://doi.org/10.2135/cropsci1998.0011183X003800030002x>
- Sparks, D. L. (2003). *Environmental soil chemistry* (2nd ed.). Academic Press. <https://doi.org/10.1016/B978-0-12-656446-4.50001-X>
- Sposito, G. (2008). *The chemistry of soils* (2nd ed.). Oxford University Press.
- Stevenson, F. J. (1994). *Humus chemistry: Genesis, composition, reactions* (2nd ed.). John Wiley & Sons.
- Van Es, H. M., Van Kessel, C., & Richter, D. D. (2002). Spatial analysis of agricultural field trials. *Agronomy Journal*, 94(1), 283–296. <https://doi.org/10.2134/agronj2002.2830>
- Van Veldhoven, P. P., & Mannaerts, G. P. (1987). Inorganic and organic phosphorus in the scheldt estuary. *Estuarine, Coastal and Shelf Science*, 25(6), 755–765.
- Verband Deutscher Landwirtschaftlicher Untersuchungs- und Forschungsanstalten (VDLUFA). (2000). *Methodenbuch band i: Die untersuchung von böden*. VDLUFA-Verlag.

10 Appendix

11 Supplements

List of Figures

1	Test of the linearized first-order kinetic model. The plot visually supports the statistical finding that many intercepts are not zero.	7
2	Non-linear first-order kinetic model fits for P desorption over time. Points represent measured data and solid lines represent the fitted model for each replicate.	8
3	Correlation between desorption-derived kinetic parameters and IEK-derived parameters. (A) Capacity parameters: Desorbable P (P_{desorb}) vs. Isotopically Exchangeable P (E_{7d}). (B) Kinetic parameters: Rate Constant (k) vs. IEK kinetic parameter (n_{1d}).	9
4	Agronomic response variables across six P fertilization treatments and six experimental sites. Data from 2017-2022.	10
5	Soil P parameters across six P fertilization treatments and six experimental sites.	11
6	Diagnostic plot for P_AAE10 (left axis) and P_CO2 (right axis) for all replicates at the Ellighausen (ELL) site, faceted by P fertilization treatment.	20

List of Tables

1	Soil characteristics of the six long-term experimental sites. Data adapted from Hirte et al. (2021).	3
2	Description of variables used in the agronomic and soil models.	5
3	Results of linear mixed-effects models predicting P parameters from intrinsic soil properties. Significance codes: ‘’ $p < 0.001$, ’’ $p < 0.01$, ’’ $p < 0.05$	12
4	Results of linear mixed-effects models predicting Site-Normalized Yield (Y_{norm}). .	13
5	Results of linear mixed-effects models predicting National-Normalized Yield (Y_{rel}). .	14
6	Results of linear mixed-effects models predicting P-Export (P_{up}).	15
7	Results of linear mixed-effects models predicting P-Balance (P_{bal}).	16



Eidgenössische Technische Hochschule Zürich
Swiss Federal Institute of Technology Zurich

Title of work:

P-release kinetic as a predictor for P-availability in the STYCS
Trials

Thesis type and date:

Master's Thesis,

Supervision:

Prof. Dr. Emmanuel Frossard
Dr. Frank Liebisch

Student:

Name: Marc Jerónimo Pérez y Roperó
E-mail: marcpe@ethz.ch
Legi-Nr.: 13-938-311

Statement regarding plagiarism:

By signing this statement, I affirm that I have read and signed the Declaration of Originality, independently produced this paper, and adhered to the general practice of source citation in this subject-area.

Declaration of Originality:

http://www.ethz.ch/faculty/exams/plagiarism/confirmation_en.pdf

Zurich, 10. 9. 2025:

My Signature